TMR
doi: 10.12032/IDR20200802006

ARTICLE

Infectious Diseases Research

Development of a Total Flavonoids Extract of *Artemisia Rupestris L.* via Nanotechnology and Its Antiviral Effect *In Vitro*

Hasimu Hamulati[1], Su-Xiang Chen[2], Zhen-Yi Gu[1], Yu-Hua Sun[1*], Tao Wang[2,3*]

[1]The Xingjian Institute of Materia Medica, Xinjiang Uygur Autonomous Region, Urumqi, P.R. China, 830004; [2]Centre for Molecular Medicine and Innovative Therapeutics, Murdoch University, Perth 6150, Australia; [3]The College of Nursing and Health, Zhengzhou University, Zhengzhou, 450001, China.

*Corresponding to: Yu-Hua Sun. he Xingjian Institute of Materia Medica, Xinjiang Uygur Autonomous Region, Urumqi, P.R. China, 830004. E-mail: 1641636482@qq.com; Tao Wang. Centre for Molecular Medicine and Innovative Therapeutics, Murdoch University, Perth 6150, Australia. E-mail: tao.wang@murdoch.edu.au.

Highlights

Nano-encapsulated Artemisia rupestris L. preparation actively targets and penetrates target cells for therapeutic purposes. Encapsulated PLGA nanoparticles allow sustained flavonoid extract of Artemisia rupestris L release. PLGA based nanotechnology endows the flavonoid extract of Artemisia rupestris L. with enhanced anti-HBV effects.

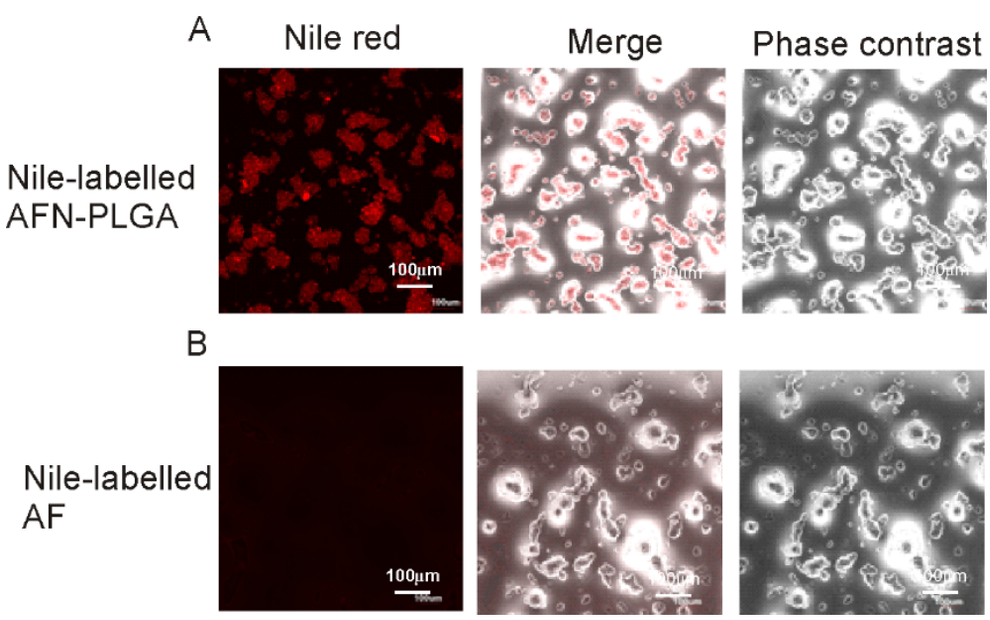

doi: 10.12032/IDR20200802006

Abstract

Objective: We aimed to develop a novel *Artemisia rupestris L*. flavonoid nano-encapsulation (AFN) preparation and evaulate its anti-hepatitis B virus (HBV) activity*in vitro*. **Methods:** First, the AFN was prepared using polylactic-co-glycolic acid (PLGA). Then, after verification of the AFN, *in vitro* anti-virus assays were conducted by: (1) assessing the inhibitory effect of AFN on the secretion of hepatitis B surface antigens (HBsAg), hepatitis B e-antigens (HBeAg), and the replication of HBV DNAin HepG2.2.15 cells; (2) analyzing the influence of AFN on the activation rate of NF-κB positive cells; and (3) evaluating the effect of AFN on the function of glutathione peroxidase (GSH-PX) enzymes located onthe HepG2.2.15 cell membrane. **Results:** Compared to the original total flavonoids extract of *Artemisia rupestris L.* (withoutnano-encapsulation), AFN preparation under the maximum non-toxic concentration effectively inhibited the secretion of HBsAg, HBeAg, and HBV DNA from HepG2.2.15 cells. At the same time, AFN preparation promoted not only the activation rate of NF-κB positive cells, but also antiviral GSH-PX enzyme function. In conclusion, nano-encapsulation of the flavonoids extract of *Artemisia rupestris L.* showed an enhanced anti-HBV effect *in vitro* compared to the original total flavonoids extract (without nano-encapsulation); therefore, nano-encapsulation has great potential for the development of a novel antiviral herbal medicine preparation with improved efficacy.

Key words: *Artemisia rupestris L.*, HBV, PLGA, Nanoparticle, Traditional medicine

Acknowledgement:

This work was supported by the Science and Technology International Cooperation Project of Xinjiang Uygur Autonomous Region of China (No. 20166015), the National Natural Science Foundation of China (No.81773175) and the China Postdoctoral Science Foundation (No. 2018M630839).

Abbreviations:

AFN, Artemisia rupestris L. flavonoid nano-encapsulation; HBV, anti-hepatitis B virus; PLGA, polylactic-co-glycolic acid; HBeAg, hepatitis B e-antigens; GSH-PX, glutathione peroxidase; DHBeAg, Duck hepatitis B e-antigens; DHBV, duck hepatitis B virus; AF, Artemisia rupestris L. flavonoids; PVA, polyvinyl alcohol; AFN, Artemisia rupestris L. flavonoid nano-encapsulation.

Competing interests:

The authors declare that they have no conflict of interest.

Citation:

Hasimu Hamulati, Su-Xiang Chen, Zhen-Yi Gu, et al. Development of a Total Flavonoids Extract of *Artemisia Rupestris L.* via Nanotechnology and Its Antiviral Effect *In Vitro*. Infectious Diseases Research 2020, 1(2): 1-10.

***Executive Editor*：**

Submitted: 16 June 2020, ***Accepted:*** 25 September 2020, ***Online:*** 02 November 2020.

doi: 10.12032/IDR20200802006

Introduction

Artemisia rupestris L. is a traditional herbal medicine that is widely used in Xinjiang (officially Xinjiang Uygur Autonomous Region of China) [1]. The application of *Artemisia rupestris L.* as a medicine was first documented in an ancient poem written by Xinjiang [1]: "there is a sprig of Artemisia at home, not afraid bitten by a snake, there is a sprig of Artemisia at home, all diseases are removed." In fact, there is also evidence of its wide application in other parts of Asia and even Europe. In 1596, *Artemisia rupestrisL.* was recorded in the Compendium of Materia Medica (also known as Bencao Gangmu or Pen-tsao Kang-mu) in the Ming Dynasty of China for the treatment of various commonly observed symptoms, such as inflammation and fever [2]. In recent years, the value of *Artemisia rupestris L.* as a medicine has been intensively exploited, and different aspects of its therapeutic value have been realized, such as antianaphylaxis, anti-virus, anti-oxidation, and immunomodulation activities [3]. Among these, the anti-hepatitis B virus (HBV) potential of *Artemisia rupestris L.* has been particularly emphasized [4]. In line with previous reports, as well as our studies, the flavonoids extract of *Artemisia rupestris L.* could effectively inhibit the key steps of HBV proliferation, including the secretion of hepatitis B surface antigens (HBsAg), hepatitis B e-antigens (HBeAg), and replication of HBV DNA. In addition, as shown in recent *in vivo* studies [5-7], the flavonoids extract of *Artemisia rupestris L.* demonstrated a potent inhibitory effect on not only the secretion of duck hepatitis B e-antigens (DHBeAg), but also the replication of duck hepatitis B virus (DHBV) DNA.

As demonstrated in our preliminary results (data not shown), the stability and clinical application of the flavonoids extract of *Artemisia rupestris L.* was compromised by its high hygroscopicity. To this end, developing liposome-based nanoparticles represents a promising strategy to resolve this problem. As shown by recent studies, by encapsulating the extract of traditional herbal medicines into liposomes, the transmembrane effect of medicines could be dramatically improved, which can lead to an increased intracellular concentration of medicines [8, 9]. In this study, to improve the stability and treatment index of the flavonoids extract of *Artemisia rupestris L.*, we employed a polylactic-co-glycolic acid (PLGA) based liposome technique to develop a novel nano-encapsulated flavonoids extract of *Artemisia rupestris L.* We comprehensively investigated the *in vitro* anti-HBV effect of the nano-encapsulated flavonoids extract of *Artemisia Rupestris L.* using the original flavonoids extract (without nano-encapsulation) as a control. Based on the preliminary results, the nano-encapsulated flavonoids extract of *Artemisia Rupestris L.* shows potential for anti-HBV therapeutic use.

Materials and Methods

1. Preparation of the total flavonoids extract of Artemisia rupestris L.

The plant powder of *Artemisia rupestris L.* (prepared by Xinjiang Uygur Autonomous Region Xinjiang West Gast Pharmaceutical Co., Ltd., Cat. 201308, verified by the Xinjiang Uygur Autonomous Region Institute of Medicine) was mixed with 50% ethanol. Extraction of total flavonoids was carried out twice by refluxing for 2 hours each time. The extracts of *Artemisia rupestris L.* flavonoids(AF) were combined and filtered and the resultant filtrates were concentrated under low pressure conditions. The *Artemisia rupestris L.* flavonoids (AF) extract was then added to a polyamide column and eluted by sequentially adding water, 10% ethanol, 30% ethanol, and 50% ethanol to the column. The eluate from the 50% ethanol was then concentrated to obtain AF. The yield of AF was determined to be 16.3%. Detailed procedures are discussed below: First, the plant (*Artemisia rupestris L.*) was crushed and then mixed with 50% ethanol, with a ratio of 1 gram per 10 mL of 50% ethanol solution; second, the above prepared solution was extracted twice by refluxing, and the time for each reflux was ~1 to 2 hours. The resultant extracts were combined and filtered to obtain a purified solution. The solution was then recovered under reduced pressure and concentrated to obtain an *Artemisia rupestris L.* extract. The relative density of the extract was ~1.20 to 1.30. The third step was to disperse the *Artemisia rupestris L.* extract in water to obtain a suspension, which was followed by centrifugation (20℃ , 4, 000 g for 10 min). The resultant supernatant was then added to a polyamide column, while the remaining *Artemisia rupestris L.* extract particles were resuspended by adding water, which was followed by vertexing and centrifugation (20℃, 4,000 g for 10 min). The resultant supernatant was transferred to the above-mentioned polyamide column as well.

The gradual dissolution step was repeated until all the *Artemisia rupestris L.* extract particles were dissolved and added to the column. After this, elution

TMR
doi: 10.12032/IDR20200802006

was performed by sequentially adding water, 10% ethanol, 30% ethanol, and 50% ethanol. The eluate was collected and concentrated to obtain the total flavonoids extract of *Artemisia rupestris L.*, with an extraction rate of 16.3%. High performance liquid chromatography (HPLC) was conducted using the Dionex ultimate 3000 system (Thermo Fisher Scientific, USA) for the quantification of AF. The mobile phase included 0.1% phosphoric acid and 0.1% methanol. The test was performed using a Nova-Pak® C18 4 μm, 3.9 × 150 mm column at a wavelength of 350 nm, temperature of 25℃ and a 50 min running time.

2 Preparation of nano-encapsulated AF

AF was dissolved in 80% methanol at a concentration of 10 mg/mL. The resultant solution was added dropwise into a PLGA nanoparticle acetone solution (90 mg/3 mL) that was continuously stirring. The resultant mixture of AF methanol solution and PLGA acetone solution was then added dropwise into 20 mL of 1% polyvinyl alcohol (PVA) to remove the acetone, followed by centrifugation at 5, 000 g and 20℃ for 10 min (to remove excessive particles) to obtain the AF/PLGA suspension. The suspension was centrifuged at 20℃, 40,000 g for 5 min. The collected AF/PLGA nanoparticles were dispersed in water and stored at −80℃. The *Artemisia rupestris L.* flavonoid nano-encapsulation (AFN) was completed when the AF encapsulated PLGA nanoparticle powder was acquired after freeze-drying.

3 Determination of encapsulation efficiency, particle size, and *in vitro* stability

To evaluate the AFN efficiency, 0.9 mg of nanoparticle powder was dissolved in 3 mL of acetone. AF was then extracted at 4° C for 72 h. This was followed by adding 2 mL of 80% methanol to dissolve the extracted AF. The suspension was centrifuged at 3, 000 g for 5 min. The AF in the suspension was measured by HPLC as detailed in the Material and Methods Section 1. To measure the particle size, the nanoparticle powder was redispersed in phosphate buffer saline (PBS, Gibco, Cat. 11510546), diluted 10 times, and then added to a suitable measuring cup to determine its particle size. To determine the stability at 3days, 6 days, and 20 days, the sample was extracted and centrifuged (4, 000 g, 5 min). The AF extract that leaked into the suspension was diluted with 80% methanol, and the AF content was measured with HPLC to determine its stability.

4 Cellular uptake assay

Similar to our previous reports [10, 11], the HepG2.2.15 cells (donated by Professor Chunyan Zhao from Jilin University) were cultured in DMEM (Gibco, Cat.31053) containing 10% FBS (Gibco, Cat.10099) in T-25 flasks. After removing the cell culture medium, the cells were washed three times with PBS using 5 mL per wash. After washing, 5 mL of the AFN culture medium (containing 200 μg/mL AF encapsulated PLGA nanoparticles) were added to the flasks and incubated at 37℃ for 3 h. After incubation, the cells were washed 3 times with PBS using 5 mL per wash. The cells were then trypsinized and centrifuged at 600 g for 5 min. After adding 5 mL of 80% methanol to the cell pellets, cells were pulverized by ultrasound for 20 min, and the suspension was centrifuged at 10,000 g for 5 min. The AF encapsulated PLGA nanoparticles in the resultant supernatant were measured with HPLC. The cells were originally ordered from ATCC.

5 Imaging assay

5.1 Preparation of fluorescently labeled drug-PLGA nanoparticles

Similar to results from a previous report [12], Nile Red (Solarbio, Cat.20160722) and AF solution in 80% methanol (1 mg Nile Red and 10 mg AF/mL) were released into PLGA solution with acetone (90 mg per 3 mL). The container of AF solution was then washed with 0.1 mL 80% methanol (Thermo Fisher Scientific, Cat. 161065) two times and the wash-over methanol was continuously added to the PLGA solution. The mixture of AF and PLGA was then added to 20 mL 1% PVA (the container of the AF/PLGA mixture was washed two times with 0.2 mL acetone and the wash-over acetone was dropped into the PVA solution as well). Acetone was removed by stirring in the fume hood for 18 h. The suspension was then centrifuged at 5,000 rpm/10 min (3,438 g/10 min) at 20℃ to remove aggregated particles and residuals. The nanoparticle suspension was ultracentrifuged at 40,000 g for 5 min (3 mL/tube) at 20℃. The resultant nanoparticle precipitate was redispersed in water (1 mL/tube) and ultracentrifuged at 40, 000 g/5 min. The nanoparticle precipitate was collected and redispersed again in water for storage at −80℃. The nanoparticle powder was obtained with freeze-drying at −80℃.

5.2 Confocal microscopy assay

Similar to the method described in a previous report [13], HepG2.2.15 cells were cultured with Fluorobrite DMEM (with 10% FBS) in a T-25 flask for

TMR
doi: 10.12032/IDR20200802006

one week before seeding at a density of 75,000 cells/cm^2 on a chamber slide (Nunc® Lab-Tek® II). After 24 hours, cells in the chamber slide were incubated with Nile Red labeled AF-PLGA nanoparticles (200 μg nanoparticles/mL in Fluorobrite DMEM containing 10% FBS and 1% penicillin-streptomycin) for 3 hours at 37℃ . After removal of the residual nanoparticle-containing culture media, cells were washed with PBS (3 times). Visualization was then performed using FluoView FV10i confocal microscopy (Excitation: 559 nm, fluorescence was detected at 570−620 nm).

6 *In vitro* anti-HBV assay

6.1 Cytotoxicity assay of HepG2.2.15 cells

According to a previous report [14], HepG2.2.15 cells were seeded on 96-well plates with 1×10^5 cells/well at 37℃ and 5% CO_2. After incubation for 12 h, AF encapsulated PLGA nanoparticles in a series of concentrations from 0.003 to 0.09 mg/mL were added to the wells with lamivudine (Fujian Guangshengtang Pharmaceutical Co., Ltd., Cat: S14202014977; 0.015625 − 0.5 mg/mL) as a positive control and AF (0.015625 − 0.5 mg/mL) as a negative control. After 72 h incubation, 10 μL of CCK-8 (Saint-Bio, Cat: 20160703) were added into each well, followed by incubation for 1 h. The OD value was tested at 450 nm using a plate reader. The TC50 (toxic concentration, 50%) and TC0 (toxic concentration, 0%) were measured with the following formulation:

$$\text{Inhibition (\%)} = \frac{\text{OD value of untreated control} - \text{OD value of treatment}}{\text{OD value of untreated control}} \times 100\%$$

6.2 The inhibition effect of AF encapsulated PLGA nanoparticles on the secretion of HBsAg, HBeAg, and the replication of HBV DNA in HepG2.2.15 cells

HepG2.2.15 cells of ~80% confluency were digested using 0.25% trypsin (Thermo Fisher Scientific, Cat: 25200056). The cells were then seeded onto 24 well plates with 10, 000 cells/mL/well. After 24 h incubation at 37℃ at 5% CO_2 with full DMEM medium, three different doses of diluted AF encapsulated PLGA nanoparticles(0.02 mg/mL, 0.01 mg/mL, and 0.005 mg/mL; TC0 = 0.02 mg/mL, 0.5×TC0 = 0.01 mg/mL, and 0.25×TC0 = 0.005 mg/mL, respectively) were added to the cells, four wells per treatment, with lamivudine serving as a control. Three days after the initial treatment (i. e., on day 4), the culture medium in different wells was replaced by fresh medium that contained different doses of the AF encapsulated PLGA nanoparticles accordingly. This replacement step was also repeated on day 5, day 6, and day 7. Seven days after the initial treatment, HBsAg and HbeAg secretion of HepG2.2.15 cells were measured with ELISA assays according to the manufacturer's specifications (Shanghai Kehua Bioengineering, Cat: 203973), while the HBV DNA replication in HepG2.2.15 cells was measured with real-time quantitative PCR (HuakeBiot. Shanghai, Cat: 32333). The forward primer was: 5'-ATCCTGCTG CTATGCCTCATCTT-3', and the reverse primer was: 5'GGCTAGTTTACTAFTFCCATTTG-3'. The PCR conditions were: 50℃ (2 min) uracil N-glycosylase incubation step, 94℃ (5 min) initial enzyme activation, followed by 40 cycles of 94℃ (10 s), and 60℃ (30 s) annealing and extension. The HBV inhibition rate was calculated using the formula shown below:

$$\text{Inhibition (\%)} = \frac{\text{OD value of untreated control} - \text{OD value of treatment}}{\text{OD value of untreated control}} \times 100\%$$

$$\text{HBV DNA Inhibition (\%)} = \frac{\text{Log OD value of untreated control} - \text{Log OD value of treatment}}{\text{Log OD value of untreated control}} \times 100\%$$

6.3 The effects of AF encapsulated PLGA nanoparticles on the activation rate of NF- κB positive cells

HepG2.2.15 cells were plated on polylysine treated glass slides and incubated at 37℃ 5% CO_2 to achieve 80% confluence. Subsequently, cells were washed with PBS and treated with different concentrations of AF encapsulated PLGA nanoparticles (0.02 mg/mL, 0.01 mg/mL, and 0.005 mg/mL), followed by 72 h incubation at 37℃ and 5% CO_2. After incubation, the activation rate of NF-κB positive cells was assessed according to the instructions for the immunohistological NF- κB 65 kit (Bosterbio USA, Cat: E2324).

6.4 Measurement of GSH-PX expression on HepG2.2.15 cell membranes

Different concentrations of AF encapsulated PLGA nanoparticles (0.02 mg/mL, 0.01 mg/mL, 0.005 mg/mL) were added to 80% confluent HepG2.2.15 cells and incubated at 37℃ and 5% CO_2 for 72 h. After incubation, the cell suspension was prepared using trypsin, with a concentration of 1×10^6

TMR
doi: 10.12032/IDR20200802006

cells/mL. Cells were then subjected to an ultrasonic machine to obtain the cell lysate. The GSH-PX was measured at 412 nm and 595 nm according to the instructions for the GSH-PX kit (GSH-PX, NanJing JianCheng Bioengineering Institute, China).

6.5 Statistics

The data analysis was performed with SPSS12.1 software. The results are expressed as the mean value ± standard deviation. Significant differences between the two groups were determined with Student's t test. *P* values <0.05 indicated a significant difference.

Results

1. Characterization of total flavonoids extract of Artemisia rupestris L.

According to the results of the HPLC assay (Figure 1), two of the reported effective components of *Artemisia rupestris L.*; i.e., vitexicarpin and artemitin, reached 4.29% and 0.29%, respectively.

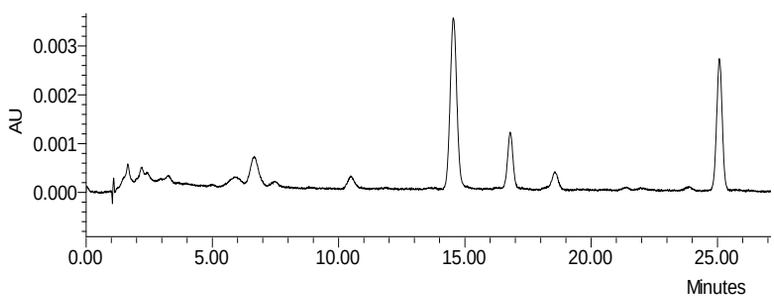

Figure 1 A representative figure of the HPLC results for *Artemisia rupestris L.* A: vitexicarpin; B: artemitin.

2 Characterization of AF encapsulated PLGA nanoparticles

As shown in Figure 2, the average particle size of AF encapsulated PLGA nanoparticles (resulting from AFN) was approximately 128.3 ± 0.5 nm, which is suitable for most delivery applications, with an encapsulation efficiency of 11.36 ± 0.22%. Importantly, analysis of the stability of AF encapsulated PLGA nanoparticles showed that even after 20 days of incubation, merely 21.87 ± 2.25% of the AF had escaped from PLGA nanoparticles into the solution (Table 1).

To effectively initiate the biological effect, a therapeutic particle needs to bind to target cells, which allows efficient uptake by the cells. To confirm the uptake of AF encapsulated PLGA nanoparticles by HepG2.2.15 cells, fluorescently labeled AF encapsulated PLGA nanoparticles were incubated with HepG2.2.15 cells and then measured with a confocal imaging assay. As shown in Figure 3, compared with the control group, AF encapsulated PLGA nanoparticles demonstrated significant cell penetration. The HPLC based cellular uptake assay (figure not shown) further indicated that AF encapsulated PLGA nanoparticles could effectively penetrate HepG2.2.15 cells. The cellular uptake rate was 1.14 ± 0.17 μg nanoparticles/mg cell protein.

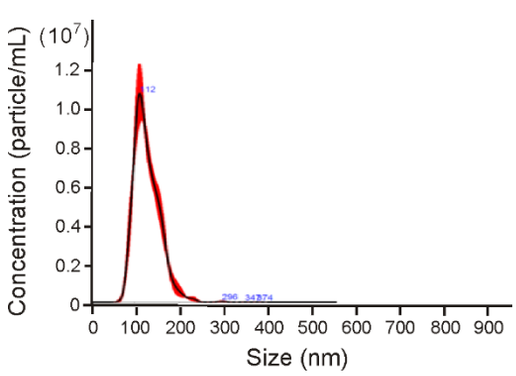

Figure 2 Representative images of the particle size of the AFN

Table 1 *In vitro* stability assay of AF encapsulated PLGA nanoparticles

Time (days)	dissolution rate
3 d	22.09 ± 2.05 %
6 d	21.63 ± 1.35 %
20 d	21.87 ± 2.25 %

Artemisia rupestris L. flavonoids(AF), **Polylactic-co-glycolic acid(PLGA)**

3 *In vitro* anti-HBV effect of AF encapsulated PLGA nanoparticles

3.1 Cytotoxicity of AF encapsulated PLGA nanoparticles to HepG2.2.15 cells

As shown in Table 2, the cytotoxicity of AF

doi: 10.12032/IDR20200802006

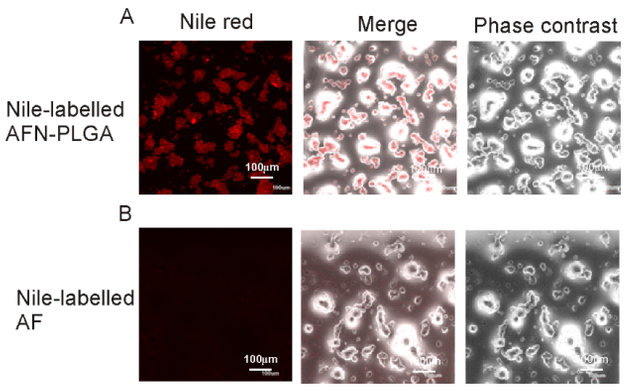

Figure 3 Confocal images of HepG2.2.15 cells that were incubated with Nile RWed labelled AF encapsulated PLGA nanoparticles

encapsulated PLGA nanoparticles to HepG2.2.15 cells demonstrated a dose-dependent mode. The dose 0.09 mg/mL had the highest inhibition rate (34.85 ± 6.243%) of HepG2.2.15 cells, while doses lower than 0.02 mg/mL did not lead to significant inhibition compared to the untreated group. Similarly, 0.5 mg/mL of lamivudine achieved 32.45 ± 2.436% inhibition of HepG2.2.15 cells. However, when the lamivudine concentration was reduced to 0.125 mg/mL, cell toxicity was not detected. In contrast, the AF group had the highest toxicity. After treating HepG2.2.15 cells with 0.5 mg/mL of AF, nearly all tested cells were eliminated (98.72 ± 8.96% inhibition). This was in agreement with our observation in a previous study, suggesting the encapsulation of drugs in nanoparticles may reduce the release of free drug molecules resulting in decreased efficacy [15]. However, as AF encapsulated PLGA nanoparticles allow sustained release of AF, the prolonged anti-virus activity of these nanoparticles was expected.

3.2 The inhibitory effects of AF encapsulated PLGA nanoparticles on HBsAg and HBeAg expression in HepG2.2.15 cells

As shown in Table 3, after a 7-day treatment, all the substances tested had an inhibitory effect on HBsAg expression of HepG2.2.15 cells (P <0.05). Although the differences in inhibitory effects resulting from different treatments were not significant, the inhibition rates (34.16 ± 5.23% and 39.37 ± 5.43%) achieved by AF encapsulated PLGA nanoparticles (0.01 mg/mL and 0.02 mg/mL, respectively) were slightly higher than that of the AF group (31.18 ± 6.24% and 0.0156 mg/mL, respectively), but slightly lower than that of the lamivudine group (41.07 ± 6.72% and 0.125 mg/mL). Regarding HBeAg expression, AF encapsulated PLGA nanoparticles had an inhibitory effect (13.32 ± 3.56% and 17.87 ± 4.44% inhibition caused by 0.012 mg/mL and 0.023 mg/mL doses, respectively) that was higher than that of the AF (6.31 ± 0.34% and 0.0156 mg/mL dose), but lower than lamivudine group (30.41 ± 6.25% and 0.125 mg/mL dose; P <0.01). The results suggested that, while AF encapsulated PLGA nanoparticles, lamivudine, and AF all had inhibitory effects on the secretion of HBsAg, there was no difference between the groups. AF encapsulated PLGA nanoparticles showed higher HBeAg inhibition than AF but lower inhibition than the lamivudine control group.

Table 2 Cytotoxicity of different treatments to HepG2.2.15 cells

Concentration (mg/mL)	OD value	Inhibition(%)	Concentration (mg/mL)	OD value	Inhibition(%)	Concentration (mg/mL)	OD value	Inhibition(%)
AFN			Lamivudine			AF		
0	3.52 ± 0.07	–	–	3.52 ± 0.07	–	–	3.52 ± 0.07	–
0.003	3.51 ± 0.09	0.049 ± 0.007	0.0156	3.51 ± 0.16	0.023 ± 0.006	0.0156	3.36 ± 0.11	4.27 ± 0.33
0.006	3.48 ± 0.07	1.059 ± 0.043	0.0312	3.51 ± 0.01	0.021 ± 0.009	0.0312	3.18 ± 0.08	9.54 ± 0.98
0.012	3.48 ± 0.14	1.131 ± 0.082	0.0625	3.51 ± 0.02	0.121 ± 0.046	0.0625	3.03 ± 0.09	13.76 ± 0.96
0.023	3.40 ± 0.08	3.363 ± 0.142	0.125	3.49 ± 0.03	0.811 ± 0.182	0.125	2.85 ± 0.04	18.89 ± 2.34
0.045	3.07 ± 0.04	12.69 ± 1.335	0.25	2.87 ± 0.07	18.25 ± 0.342	0.25	1.22 ± 0.06	65.25 ± 5.23
0.09	2.29 ± 0.16	34.85 ± 6.243	0.50	2.37 ± 0.06	32.45 ± 2.436	0.50	0.33 ± 0.04	98.72 ± 8.96

3.3 The inhibition effects of AF encapsulated PLGA nanoparticles on HBV-DNA replication in HepG2.2.15 cells

As shown in Table 4, after 7 days of treatment, AF encapsulated PLGA nanoparticles achieved around 15.72 ± 2.11% and 9.22 ± 1.27% inhibition of HBV-DNA (p <0.05) at the concentrations of 0.02 mg/mL and 0.01 mg/mL, respectively, which were significantly higher than the concentrations (6.90 ± 0.76%) inhibited by AF (0.0156 mg/mL).

doi: 10.12032/IDR20200802006

Table 3 Inhibition of different treatments to HBsAg and HBeAg expression in HepG2.2.15 cells after 7 days of treatment

Treatment	Concentration (mg/mL)	HBsAg		HBeAg	
		OD value	Inhibition (%)	OD value	Inhibition (%)
Untreated		3.692 ± 0.070	–	2.306 ± 0.068	–
AFN	0.005	2.670 ± 0.029*	27.68 ± 3.46*	2.147 ± 0.189	6.80 ± 1.22
	0.01	2.431 ± 0.187*	34.16 ± 5.23*	1.999 ± 0.139*#++	13.32 ± 3.56*#++
	0.02	2.239 ± 0.116*	39.37 ± 5.43*	1.894 ± 0.123*##++	17.87 ± 4.44*##++
Lamivudine	0.125	2.176 ± 0.056*	41.07 ± 6.72*	1.605 ± 0.062*	30.41 ± 6.25*
AF	0.0156	2.541 ± 0.062*	31.18 ± 6.24*	2.161 ± 0.050	6.31 ± 0.34

* P <0.05, vs untreated group; # P <0.05, vs AF group; ## P <0.01, vs AF group;++P <0.01, vs lamivudine group

Table 4 Inhibition of different treatments on HBV-DNA replication in HepG2.2.15 cells after 7 days treatment

Treatment	Concentration (mg/mL)	HBV-DNA	
		Log copy	Inhibition (%)
Untreated		4.617 ± 0.221	–
AFN	0.005	4.583 ± 0.211	0.74 ± 0.03
	0.01	4.192 ± 0.249*++	9.22 ± 1.27*++
Lamivudine	0.02	3.891 ± 0.211*#+	15.72 ± 2.11*#+
AF	0.125	3.581 ± 0.073*	22.44 ± 6.53*
	0.0156	4.618 ± 0.144	6.90 ± 0.76

* P <0.05, vs untreated group; #P <0.05, vs AF group; +P <0.05, vs lamivudine group,++P <0.01, vs lamivudine group

3.4 The effect of AF encapsulated PLGA nanoparticles on NF-κB activation of HepG2.2.15 cells

As shown in Table 5, compared with untreated controls (7.08% ± 1.35%), treatment of AF encapsulated PLGA nanoparticles demonstrated significantly higher NF-κB activation in HepG2.2.15 cells in all the tested concentration groups. At a concentration of 0.01 mg/mL (11.12% ± 1.75%) and 0.02 mg/mL (14.04% ± 2.8%), AF encapsulated PLGA nanoparticles had higher NF-κB activation than that of the AF treatment group (8.32 ± 2.37, 0.0156 mg/mL). Although the lamivudine group led to higher cellular NF-κB activation (16.95% ± 2.75%) than the AF encapsulated PLGA nanoparticle group, a statistically significant difference was not found.

3.5 The effect of AF encapsulated PLGA nanoparticles on the activity of GSH-PX on HepG2.2.15 cell membranes

As shown in Table 5, GSH-PX expression showed a significant increase after treatment with AF encapsulated PLGA nanoparticles (e.g., 71.44 ± 12.96, 0.02 mg/mL) compared to the untreated controls (37.08 ± 9.83%). Meanwhile, the treatment with different doses of AF encapsulated PLGA nanoparticles (58.75 ± 9.58, 0.01mg/mL; 71.44 ± 12.96, 0.02 mg/mL) achieved much higher GSH-PX activity in HepG2.2.15 cells compared to the AF treatment (47.25 ± 6.54, 0.0156 mg/mL). In addition, HepG2.2.15 cells treated byAF encapsulated PLGA nanoparticles (71.44 ± 12.96, 0.02 mg/mL) and lamivudine (85.9 ± 11.19, 0.125 mg/mL) showed comparable GSH-PX activity in contrast to the untreated group (37.08 ± 9.83).

Table 5 The effect of AF encapsulated PLGA nanoparticles on NF-κB activity inHepG2.2.15 cells

Treatment	Concentration (mg/mL)	NF-κB activation rate (%)	GSH-PX activity
Untreated	–	7.08 ± 1.35	37.08 ± 9.83
AFN	0.005	10.82 ± 1.89**	54.36 ± 5.85**
	0.01	11.12 ± 1.75**#	58.75 ± 9.58*#+
	0.02	14.04 ± 2.8**##	71.44 ± 12.96**##
Lamivudine	0.125	16.95 ± 2.75**	85.9 ± 11.19**
AF	0.0156	8.32 ± 2.37*	47.25 ± 6.54*

** P <0.01,vs untreated; # P <0.05, vs AF treatment; ## P <0.01, vs AF treatment.

4 Discussion

Analysis of drug action indicators plays a key role in the development of new drugs [16]. HBsAg and HBeAg are soluble proteins encoded by the HBV genome. They are expressed in HepG2.2.15 cells (HepG2.2.15 cells are derived from HepG2 liver hepatocellular cells transfected by the HBV genome) and can be detected in the cell culture supernatant of HepG2.2.15 cells, which can reflect the replication of HBV [17]. As shown in previous studies, hepatocytes are not only passive target cells that are attacked by lymphocytes after a HBV infection, but they are also active immune effector cells that can directly clear HBV from the body. The HepG2 cell line can express a variety of cytokines, such as interferons that directly

TMR
doi: 10.12032/IDR20200802006

inhibit viral replication. The activation of NF-κB leads to the activation and release of cytokines (such as interferon-γ), increased activity of natural killer cells, and enhanced immune function. This thereby plays a key role in the outcome of HBV infection [5, 18, 19]. Lipid nanoparticles possess enhanced drug-loading capabilities that improve drug solubility, bioavailability, and stability. Therefore, lipid nanoparticles can be used for controlled-release and targeted drug delivery [15, 20, 21]. In recent years, lipid nanoparticles have been widely used in traditional Chinese herbal medicine preparations, especially the encapsulation of the active ingredients of these herbal medicines [22]. At present, liposome-based traditional Chinese herbal medicine preparations have been intensively investigated [23]. It has been found that this type of preparation can improve the solubility of the therapeutically active components (compounds) of herbal medicines. As a kind of lipophilic material, liposomes can increase cell membrane permeability thereby allowing efficient penetration of drug compounds encapsulated in liposomes through the cell membrane, which increases the intracellular concentration of drug compounds, thereby improving drug utilization [24-26].

Artemisia rupestris L. has been used as an herbal medicine in China for centuries and it holds great potential for medical applications in various fields due to its therapeutic capabilities, including anti-inflammation, anti-allergy, liver-protection, anti-virus, bacteriostatics, and anti-tumor effects. In recent years, the chemical constituents of *Artemisia rupestris L.* have been comprehensively studied. Studies have shown that the pharmacological effects of *Artemisia rupestris L.* are due to mainly flavonoids, sesquiterpenes, alkaloids, and polysaccharides. Among them, flavonoid compounds including 6'-demethoxy-4'-O-methyl protonone-7'-O- β -D glucoside, vitexin, isoranin, locustin, yanaisu, anisodamine-3, and 3′, 4′-trimethyl ether have been identified [27, 28]. For anti-HBV effects of *Artemisia rupestris L.*, the roles of vitexin and locustin were especially emphasized [29, 30].

In this study, we extracted total flavonoid contents from *Artemisia rupestris L.* and encapsulated them into PLGA nanoparticles. The resultant AF encapsulated PLGA nanoparticles achieved improved inhibitory effects on HBV replication (indicated by the expression of HBsAg and HBeAg, and replication of HBV DNA) *in vitro* compared to the AF treatment (total flavonoid extracts without nano-encapsulation by PLGA nanoparticles) using treatment with lamivudine, an antiretroviral medicine as a positive control. Furthermore, treatment of AF encapsulated PLGA nanoparticles increased the immune responses of HepG2.2.15 cells (indicated by NF-κB activation andGSH-PX activity) to a higher extent compared to the AF treatment. While the former inhibition of HBV replication *in vitro* suggests a direct anti-HBV effect, the latter activation of NF-κB and GSH-PX provides evidence of indirect antiviraleffects. In addition, excellent stability of AF encapsulated PLGA nanoparticles (*in vitro* stability was ensured even after 20 days) is expected to allow controlled-release of AF, which may achieve sustained efficacy and reduced side effects as well. Although this is only a preliminary study, further investigation to analyze individual compounds of the total flavonoids extract of *Artemisia Rupestris L.* has been scheduled. However, based on the results, we firmly suggest that nano-encapsulation can be a practical way to improve the therapeutic efficacy of traditional herbal medicines.

Reference

1. Zhang A., et al., The effect of aqueous extract of Xinjiang Artemisia rupestris L. (an influenza virus vaccine adjuvant) on enhancing immune responses and reducing antigen dose required for immunity. PLoS One, 2017. 12(8): p. e0183720.
2. Liu X. C., et al., Identification of repellent and insecticidal constituents of the essential oil of Artemisia rupestris L. aerial parts against Liposcelis bostrychophila Badonnel. Molecules, 2013. 18(9): p. 10733-46.
3. Nigam M., et al., Bioactive Compounds and Health Benefits of Artemisia Species. Nat. Prod. Commun., 2019. 14(7).
4. Geng C. A., et al., Anti-hepatitis B virus effects of the traditional Chinese herb Artemisia capillaris and its active enynes. J Ethnopharmacol, 2018. 224: p. 283-289.
5. Geng C. A., et al., Three new anti-HBV active constituents from the traditional Chinese herb of Yin-Chen (Artemisia scoparia). J Ethnopharmacol, 2015. 176: p. 109-17.
6. Lan J. E., et al., Flavonoids from Artemisia rupestris and their synergistic antibacterial effects on drug-resistant Staphylococcus aureus. Nat. Prod. Res., 2019.
7. Geng, ChenC. A. and J. J., The Progress of Anti-HBV Constituents from Medicinal Plants in China. Nat Prod Bioprospect, 2018. 8(4): p. 227-244.

TMR
doi: 10.12032/IDR20200802006

8. GE Hai-tao, U. K. -q., Wang Xiao-lei, Effects of Compound Artemisia Rupestris Tablet on Anti-inflammatory and Immune Function in Mice. Chinese and Foreign Medical Research, 2014. 12 (8): p. 3.
9. Yong J. P., LuC. Z., and AisaH. A., Advances in Studies on the Rupestonic Acid Derivatives as Anti-influenza Agents. Mini-Reviews in Medicinal Chemistry, 2013. 13(2): p. 310-315.
10. Wang T., et al., EpCAM Aptamer-mediated Survivin Silencing Sensitized Cancer Stem Cells to Doxorubicin in a Breast Cancer Model. Theranostics, 2015. 5(12): p. 1456-72.
11. Wang T., RahimizadehK., and VeeduR. N., Development of a Novel DNA Oligonucleotide Targeting Low-Density Lipoprotein Receptor. Mol Ther Nucleic Acids, 2020. 19: p. 190-198.
12. Tran P. H. L., et al., Development of a nanoamorphous exosomal delivery system as an effective biological platform for improved encapsulation of hydrophobic drugs. Int J Pharm, 2019. 566: p. 697-707.
13. Wang T., et al., Efficient Epidermal Growth Factor Receptor Targeting Oligonucleotide as a Potential Molecule for Targeted Cancer Therapy. Int. J. Mol. Sci., 2019. 20(19).
14. Wang T., et al., Systematic Screening of Commonly Used Commercial Transfection Reagents towards Efficient Transfection of Single-Stranded Oligonucleotides. Molecules, 2018. 23(10).
15. Lin J., et al., Improved Efficacy and Reduced Toxicity of Doxorubicin Encapsulated in Sulfatide-Containing Nanoliposome in a Glioma Model. Plos One, 2014. 9(7).
16. Xue Yang X.-Y.L., Annual advances in traditional medicine for tumor therapy in 2019. Tradit. Med. Res., 2020. 5(2): p. 90-107.
17. Liaw, Y.F., *Clinical utility of HBV surface antigen quantification in HBV e antigen-negative chronic HBV infection*. Nat Rev Gastroenterol Hepatol, 2019. 16(10): p. 631-641.
18. Williams, N., *Flu pandemic fears continue*. Curr Biol, 2005. 15(9): p. R313-4.
19. Cheung C.Y., et al., Induction of proinflammatory cytokines in human macrophages by influenza A (H5*N1) viruses: a mechanism for the unusual severity of human disease?* Lancet, 2002. 360 (9348): p. 1831-1837.
20. Agarwal, R., et al., *Liposomes in topical ophthalmic drug delivery: an update*. Drug Deliv, 2016. 23(4): p. 1075-91.
21. Wang, T., et al., *Cancer stem cell targeted therapy: progress amid controversies*. Oncotarget, 2015. 6(42): p. 44191-206.
22. Jing-Na Zhou G.-W.Z., Antitumor applications of nano-traditional Chinese medicine. Tradit. Med. Res., 2019. 4(5): p. 224-226.
23. Chaoliang Tang H. L., Junmou Hong, Xiaoqing Chai, Application of nanoparticles in the early diagnosis and treatment of tumors: current status and progress. Tradit. Med. Res., 2020. 5(1): p. 34-43.
24. Goncalves L.M.D., et al., Development of solid lipid nanoparticles as carriers for improving oral bioavailability of glibenclamide. EurJ PharmBiopharm, 2016. 102: p. 41-50.
25. Schubert, M. A. and C. C. Muller-Goymann, *Characterisation of surface-modified solid lipid nanoparticles (SLN): influence of lecithin and nonionic emulsifier.* Eur J Pharm Biopharm, 2005. 61(1-2): p. 77-86.
26. Sinico C., et al., Liposomal incorporation of Artemisia arborescens L. essential oil and in vitro antiviral activity. Eur J Pharm Biopharm, 2005. 59 (1): p. 161-8.
27. Zeng Y. T., et al., Antitumor and apoptotic activities of the chemical constituents from the ethyl acetate extract of Artemisia indica. Mol Med Rep, 2015. 11(3): p. 2234-2240.
28. He F., et al., Rupestines F-M, new guaipyridine sesquiterpene alkaloids from Artemisia rupestris. Chem Pharm Bull (Tokyo), 2012. 60(2): p. 213-8.
29. Liu M. M., et al., Discovery of flavonoid derivatives as anti-HCV agents via pharmacophore search combining molecular docking strategy. Eur. J. Med. Chem, 2012. 52: p. 33-43.
30. Huang, X., et al., *Chemical composition and bioactivity of the essential oil from Artemisia lavandulaefolia (Asteraceae) on Plutella xylostella (Lepidoptera: Plutellidae)*. FlaEntomol, 2018. 101(1): p. 44-48.

2020 by the authors. Licensee TMR, Auckland, New Zealand. This article is an open access article distributed under the terms and conditions of the Creative Commons Attribution (CC BY) license (http://creativecommons.org/licenses/by/4.0/)